Cancer Cell
Article

Targeting of the Tumor Suppressor GRHL3 by a miR-21-Dependent Proto-Oncogenic Network Results in PTEN Loss and Tumorigenesis

Charbel Darido,[1] Smitha R. Georgy,[1] Tomasz Wilanowski,[2] Sebastian Dworkin,[1] Alana Auden,[1] Quan Zhao,[1] Gerhard Rank,[1] Seema Srivastava,[1] Moira J. Finlay,[3] Anthony T. Papenfuss,[4] Pier Paolo Pandolfi,[5,6] Richard B. Pearson,[7,8,9] and Stephen M. Jane[1,10,*]
[1]Department of Medicine, Monash University Central Clinical School, Prahran, Victoria 3181, Australia
[2]Laboratory of Signal Transduction, Nencki Institute of Experimental Biology, Polish Academy of Sciences, 02-093 Warsaw, Poland
[3]Department of Pathology, Royal Melbourne Hospital, Parkville, Victoria 3050, Australia
[4]Division of Bioinformatics, The Walter and Eliza Hall Institute, Parkville, Victoria 3050, Australia
[5]Cancer Genetics Program
[6]Department of Medicine and Pathology
Beth Israel Deaconess Medical Center, Harvard Medical School, Boston, MA 02215, USA
[7]Growth Control and Differentiation Program, Peter MacCallum Cancer Centre, Melbourne, Victoria 3002, Australia
[8]Department of Biochemistry and Molecular Biology
[9]Department of Medicine
University of Melbourne, Parkville, Victoria 3050, Australia
[10]Alfred Hospital, Prahran, Victoria 3181, Australia
*Correspondence: stephen.jane@monash.edu
DOI 10.1016/j.ccr.2011.10.014

SUMMARY

Despite its prevalence, the molecular basis of squamous cell carcinoma (SCC) remains poorly understood. Here, we identify the developmental transcription factor *Grhl3* as a potent tumor suppressor of SCC in mice, and demonstrate that targeting of *Grhl3* by a miR-21-dependent proto-oncogenic network underpins SCC in humans. Deletion of *Grhl3* in adult epidermis evokes loss of expression of PTEN, a direct GRHL3 target, resulting in aggressive SCC induced by activation of PI3K/AKT/mTOR signaling. Restoration of *Pten* expression completely abrogates SCC formation. Reduced levels of *GRHL3* and *PTEN* are evident in human skin, and head and neck SCC, associated with increased expression of miR-21, which targets both tumor suppressors. Our data define the *GRHL3-PTEN* axis as a critical tumor suppressor pathway in SCC.

INTRODUCTION

The mammalian epidermis serves as an impermeable barrier, protecting the organism from the hostile external environment. It is maintained by a self-renewal process in which keratinocytes proliferating in the basal layer detach from the underlying basement membrane, withdraw from the cell cycle, and differentiate while migrating toward the skin surface (Clayton et al., 2007; Fuchs and Raghavan, 2002; Watt, 2001). Perturbation of the balance between keratinocyte proliferation and differentiation underpins a wide range of skin pathologies. When disrupted during embryogenesis, it results in a markedly thickened epidermis with altered expression of structural proteins leading to a failure of skin barrier formation (Koster, 2009). In adults it is the central tenet of various disease states, including the epidermal cancers, the most common of all human tumors (Alam and Ratner, 2001; Rogers et al., 2010).

Although abnormal activation of the sonic hedgehog/patched pathway is critical for the proliferation/differentiation imbalance in basal cell carcinoma (Wetmore, 2003), the molecular basis

Significance

The molecular basis of SCC is poorly understood. Here, we identify the developmental transcription factor GRHL3 as a potent tumor suppressor in SCC in both humans and mice. We define Pten as the critical downstream effector of Grhl3 tumor suppressor activity, providing the elusive explanation for the low levels of Pten expression in SCC that occur in the absence of genetic or epigenetic alterations to the gene. In humans we identify a miR-21 proto-oncogenic network that synchronously targets GRHL3 and PTEN leading to amplification of PI3K/AKT/mTOR signaling and induction of SCC of both skin, and head and neck origins. We demonstrate that *Grhl3/PTEN*-deficient SCC displays an oncogene addiction to the PI3K/AKT-signaling pathway, with profound downregulation of the MAPK/ERK pathway.

of squamous cell carcinoma (SCC) has been less well defined (Ridky and Khavari, 2004). Studies in human tissue models have provided evidence that activation of Ras signaling, in concert with inhibition of NF-κB function, is sufficient for malignant transformation of keratinocytes. In human tumors, *Ras* activation is most frequently due to mutations in codon 12, 13, or 61 of one of the three *Ras* genes (Bos, 1989). However, mutations in *Ras* isoforms are found in only 22% of SCCs (Khavari and Rinn, 2007), although some tumors can display increased levels of active Ras-GTP in the absence of a mutation (Dajee et al., 2003). In the classical skin chemical carcinogenesis model in mice, mutations in codon 61 of the *H-Ras* gene induced by the topical application of 7, 12-dimethylbenz[a]anthracene (DMBA) predominate (Abel et al., 2009). Activated Ras stimulates multiple effectors including the Raf/MEK/ERK pathway, the phosphatidylinositol 3-kinase (PI3K)/AKT/mTOR pathway, and the guanine nucleotide exchange factors (Repasky et al., 2004). Each of these has been clearly implicated in the pathogenesis of keratinocyte hyperproliferation and dedifferentiation, and/or overt SCC in mice (González-García et al., 2005; Scholl et al., 2007; Segrelles et al., 2007), although data from primary human samples are less compelling, or completely lacking.

An alternate mechanism for activation of PI3K/AKT/mTOR signaling in SCC is through loss of expression of the phosphatase and tensin homolog (*PTEN*) tumor suppressor gene. Previous studies have suggested that activation of *H-ras* and complete loss of *Pten* are mutually exclusive in skin carcinomas (Mao et al., 2004). *PTEN* acts as the most important negative regulator of the PI3K pathway, converting phosphatidylinositol 3,4,5-triphosphate (PIP_3), the product of activated PI3K, to phosphatidylinositol 4,5-biphosphate (PIP_2) (Stambolic et al., 1998; Maehama and Dixon, 1998). Inactivation of *PTEN* leads to accumulation of PIP_3, and as a consequence, increased activity of the serine/threonine kinases PDK1 and AKT, which promote cellular survival, cell cycle progression and growth, angiogenesis, and cellular metabolism through phosphorylation of numerous diverse cellular substrates (Manning and Cantley, 2007). AKT activation also leads to activation of the mTOR kinase complex 1 (mTORC1), resulting in activation of S6K1 and phosphorylation of 4EBP1, and enhanced protein translation through multiple effector pathways. *PTEN* has been implicated in SCC in both humans and mice (Ming and He, 2009; Suzuki et al., 2003). Despite this, somatic mutations, gene deletions, and promoter hypermethylation of PTEN have not been detected in human SCC, suggesting that other mechanisms of inactivating the gene may be involved in SCC pathogenesis (Ming and He, 2009).

Another tumor suppressor of SCC in humans and mice is IκB kinase α (IKKα) (Liu et al., 2006, 2008; Maeda et al., 2007). Adult mice with a targeted deletion of this gene in keratinocytes develop epidermal hyperproliferation, perturbed expression of differentiation markers, and ultimately, spontaneous SCC (Liu et al., 2008). Constitutive deletion of IKKα during embryogenesis leads to a thickened and undifferentiated epidermis, with neonates dying of dehydration due to a profound skin barrier defect (Hu et al., 1999; Takeda et al., 1999). These findings are of considerable interest because they demonstrate that a key regulator of keratinocyte proliferation/differentiation balance during embryonic development can also play a major role as a tumor suppressor in adulthood (Descargues et al., 2008).

We have previously shown that mice lacking the *Grainy head-like 3* (*Grhl3*) gene exhibit a markedly thickened epidermis, perturbed expression of multiple epidermal differentiation markers, and defective skin barrier formation, with newborn pups dying of dehydration (Ting et al., 2005; Yu et al., 2006). *Grhl3* is a member of a highly conserved family of transcription factors critical for epidermal development and homeostasis across a wide range of species (Jane et al., 2005; Venkatesan et al., 2003; Wilanowski et al., 2002). Expression of this gene is largely confined to the surface ectoderm during embryogenesis, and in adulthood occurs in tissues that arise from this embryonic layer, including the skin, and lining of the oral cavity. The antecedent member of this family in *Drosophila*, *grainy head* (*grh*) plays central roles in cuticle formation and repair (Bray and Kafatos, 1991; Mace et al., 2005). In view of the essential role played by *Grhl3* in maintaining the proliferation/differentiation balance in epidermal ontogeny, and the burgeoning links between conserved developmental genes and cancer (Dean, 1998), we have further investigated the role of *Grhl3* in adult skin homeostasis and skin cancer development.

RESULTS

Grhl3 Deletion during Embryogenesis Causes Epidermal Keratinocyte Hyperproliferation

Our initial experiments focused on the proliferative potential of keratinocytes in the *Grhl3* null mice. The epidermis in embryonic day (E) 18.5 $Grhl3^{-/-}$ animals was markedly thickened (Figure 1A), and expression of the proliferative marker PCNA was expanded compared to wild-type epidermis, with mitotic cells extending into the suprabasal layers (Figure 1B). This hyperproliferation was cell intrinsic because keratinocytes cultured from E18.5 $Grhl3^{-/-}$embryos grew more rapidly than the wild-type controls (Figure 1C), and displayed loss of cell-cell contact inhibition, forming heaped up pseudo-tumors in the culture dish (Figure 1D). They also displayed increased colony numbers in soft agar (Figure 1E), strengthening the possibility that *Grhl3* could play a tumor suppressor role in skin cancer in adult mice. To investigate this, we generated mice carrying a conditionally targetable *Grhl3* allele, with *loxP* sites flanking exons 2 and 4 of the gene (see Figures S1A–S1C available online and Experimental Procedures). Mice homozygous for the floxed alleles ($Grhl3^{fl/fl}$) were healthy and fertile, and when crossed with $Grhl3^{+/-}$ mice carrying a B6-*Cre* transgene expressed at the two-cell stage of development, generated $Grhl3^{\Delta/-}$/B6-*Cre*+ mice (where Δ is the deleted floxed allele) that phenocopied the *Grhl3* null animals (Ting et al., 2003, 2005) (data not shown). To delete *Grhl3* in the skin, we crossed $Grhl3^{fl/-}$ mice with a line carrying a keratin (K) 14-driven *Cre* transgene. Although patchy deletion in the epidermis has been reported with this line as early as E13.5 (using a ROSA cross) (Jonkers et al., 2001), analysis of the epidermis in E18.5 $Grhl3^{fl/-}$/*K14Cre*+ embryos revealed less than 20% deletion (Figure S1D), and all E18.5 $Grhl3^{fl/-}$/*K14Cre*+ embryos displayed normal skin barrier formation (data not shown). High levels of deletion (>95%) of the $Grhl3^{fl}$ allele were only detected after birth (from P1 onward) (Figure S1D), and consistent with this, expression of *Grhl3* in the deleted skin was markedly reduced (Figure S1E). Interestingly, the $Grhl3^{\Delta/-}$/*K14Cre*+ mice displayed no defect in skin barrier

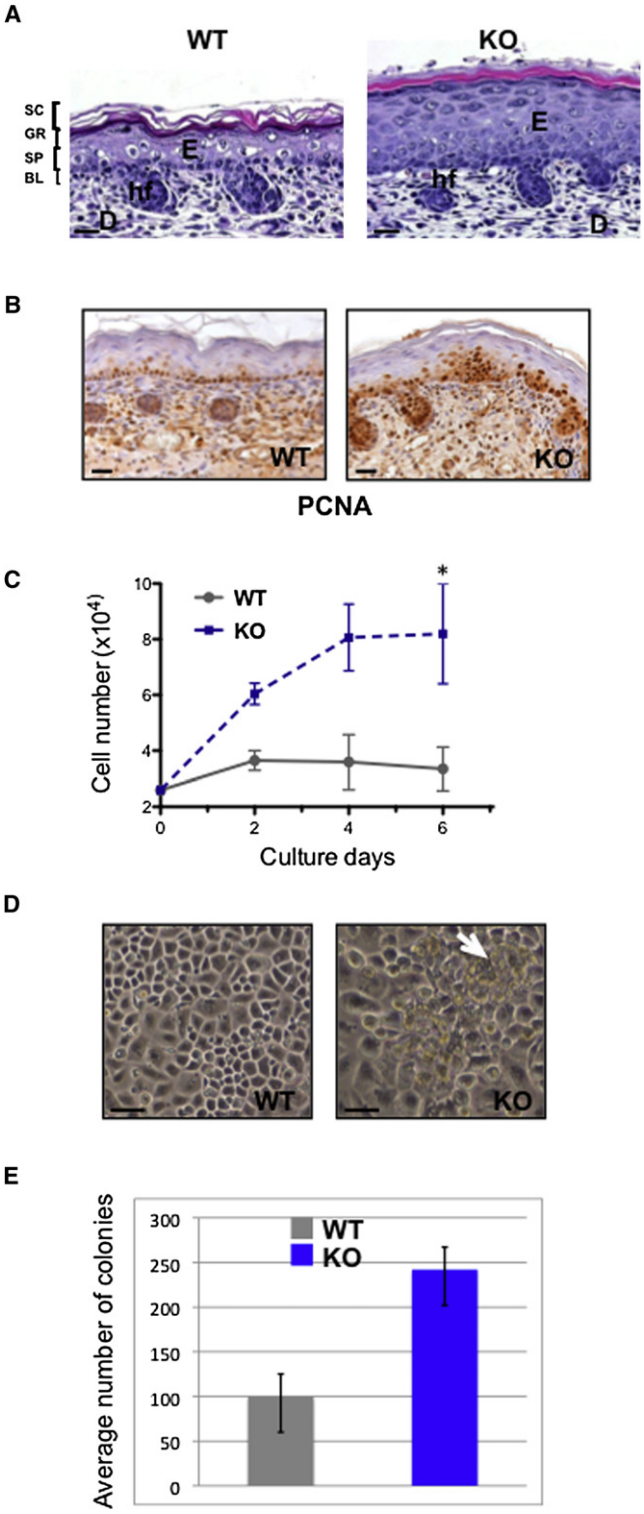

Figure 1. Hyperproliferation of *Grhl3* Null Keratinocytes

(A and B) Histology and PCNA IHC on skin from E18.5 wild-type (WT) and *Grhl3*$^{-/-}$ (KO) embryos. E, epidermis; D, dermis; hf, hair follicle. Scale bars correspond to 50 μm.

(C–E) Cell numbers, appearance, and soft agar colony numbers of cultured keratinocytes from WT and KO E18.5 embryos. For keratinocyte cultures, 2.6 × 10^4 cells were seeded at day 0. For soft agar, 3.4 × 10^5 cells were seeded at day 0. Arrow shows pseudo-tumor. The differences in cell number were statistically significant ($p < 0.03$) using a Student's t test. Error bars represent the standard deviation (±SD). The scale bars in (D) correspond to 50 μm.

function at P7 (data not shown), and appeared normal at 8 weeks, indicating that although *Grhl3* was essential for establishment of the barrier in utero, it was not essential for its maintenance after birth.

Mice with *Grhl3* Deletion in Keratinocytes Display Enhanced Susceptibility to Chemical-Induced and Spontaneous SCC

To examine the role of *Grhl3* in skin tumorigenesis, we used a well-established chemical carcinogenesis protocol on cohorts of *Grhl3*$^{\Delta/-}$*/K14Cre*+ mice and wild-type controls (n = 18 in each group), in which tumors were initiated by topical application of DMBA, and promoted by twice-weekly 12-*O*-tetradecanoylphorbol-13-acetate (TPA) (Abel et al., 2009). Papilloma formation was observed within 4 weeks in the *Grhl3*$^{\Delta/-}$*/K14Cre*+ animals, but not until 13 weeks in any controls, by which time 100% of the mutant mice had developed tumors (Figure 2A). The rapidity of tumor formation was striking; particularly because the background strain of the mutant animals (C57Bl/6) is notoriously resistant to chemical-induced tumor formation (Sundberg et al., 1997). Total tumor numbers were also markedly higher in the mutant versus wild-type mice (Figure 2B), and many of the papillomas progressed on to form SCCs (Figure 2C), a rare event in the wild-type mice. The SCCs grew rapidly and were often multiple (Figures 2D), and histologically were poorly differentiated with numerous mitoses (Figure 2E). The epidermis adjacent to the tumors was markedly thickened compared to wild-type mice and resembled the epidermis from *Grhl3* null embryos (Figure S2, H&E). Consistent with this, perturbed expression of the terminal differentiation markers filaggrin and involucrin, and the Ks 5, 6, and 10 in the *Grhl3*-deleted adult skin also mirrored the changes observed in the *Grhl3* null embryos (Figure S2A) (Yu et al., 2006). Expression of *Grhl3* was markedly reduced in treated skin prior to the onset of tumors, and completely absent in both papillomas and SCCs from the *Grhl3*$^{\Delta/-}$*/K14Cre*+ mice (Figure 2F). Tumors were also observed with high frequency in *Grhl3*$^{\Delta/-}$*/K14Cre*+ animals, but not wild-type controls (n = 10 in each group) treated with TPA alone (Figure 2G; Figure S2B), suggesting that loss of *Grhl3* is sufficient for disease initiation. With aging, 100% of the untreated *Grhl3*$^{\Delta/-}$*/K14Cre*+ mice developed epidermal hyperplasia and spontaneous tumors that were predominantly squamous papillomas or carcinomas affecting the snout and neck (Figure 2H). Identical findings were obtained when mouse mammary tumor virus (MMTV)-*Cre* transgenic mice were used to delete *Grhl3* in keratinocytes (data not shown) (Liu et al., 2008). These snout and neck tumors in both *Grhl3*$^{\Delta/-}$ lines phenocopied changes observed in mice with a keratinocyte-specific deficiency of the tumor suppressor, *Pten* (Suzuki et al., 2003).

PTEN Is a Direct Transcriptional Target Gene of GRHL3

The DNA consensus-binding site for human GRHL3 and its *Drosophila* homolog, *grh*, has been conserved across 700 million years of evolution (Ting et al., 2005). On this basis we predicted

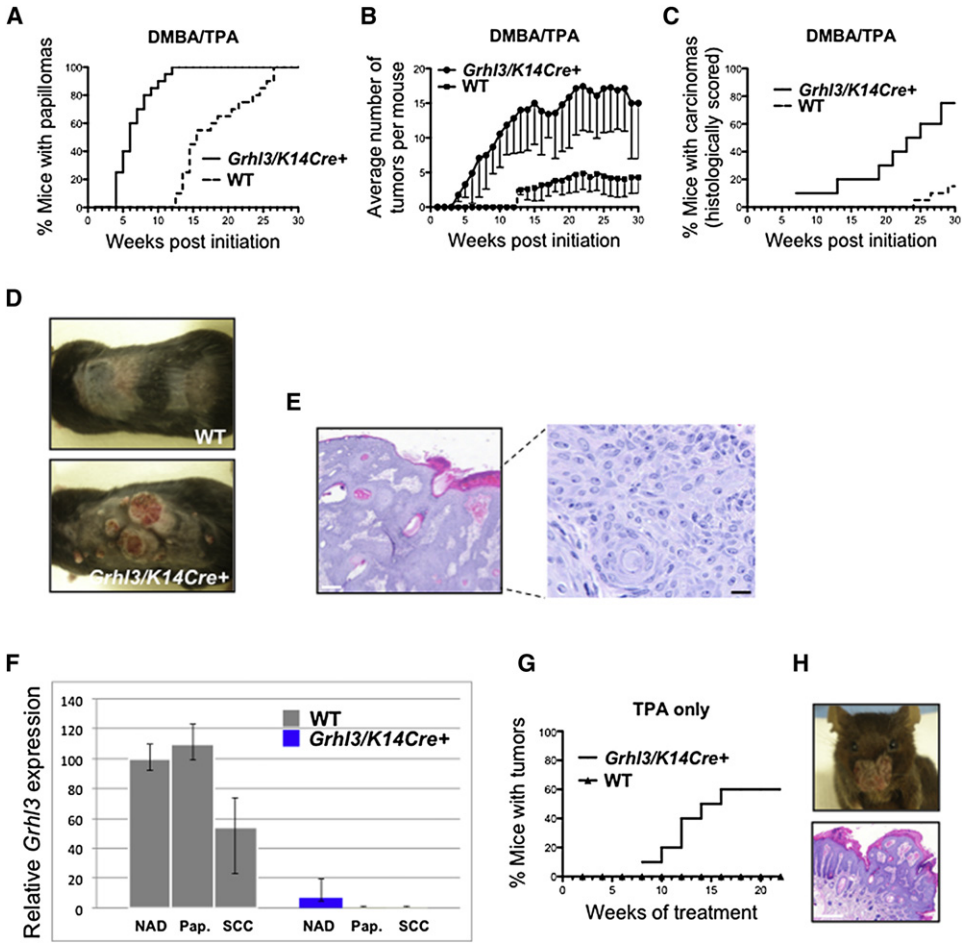

Figure 2. *Grhl3* Functions as a Tumor Suppressor in Mice

(A–C) Tumor incidence, number, and malignant potential in DMBA/TPA-treated WT and *Grhl3*$^{\Delta/-}$/*K14Cre*+ mice. The differences in tumor incidence ($p < 0.001$), number ($p < 0.05$), and malignant potential ($p < 0.001$) were statistically significant using a Student's t test.

(D) Macroscopic appearance of DMBA/TPA-treated WT and *Grhl3*$^{\Delta/-}$/*K14Cre*+ mice at 15 weeks.

(E) Histology of SCC at low (left panel) and high magnification from DMBA/TPA-treated *Grhl3*$^{\Delta/-}$/*K14Cre*+ mice. (See also Figure S2A.)

(F) *Grhl3* expression levels by Q-RT-PCR in normal skin (NAD), papillomas (pap), and SCCs from DMBA/TPA-treated WT and *Grhl3*$^{\Delta/-}$/*K14Cre*+ mice. The differences in expression between wild-type and *Grhl3*$^{\Delta/-}$/*K14Cre*+-derived tissues were significant ($p < 0.001$) using a Student's t test. Mean of three independent experiments ±SD.

(G) Tumor incidence in WT and *Grhl3*$^{\Delta/-}$/*K14Cre*+ mice treated with TPA alone.

(H) Macroscopic and microscopic appearance of spontaneous snout tumor in *Grhl3*$^{\Delta/-}$/*K14Cre*+ mice. (See also Figure S2B.)

Scale bars correspond to 200 μm (white) and 50 μm (black).

that GRHL3 target genes should contain this motif conserved across a wide range of species. Therefore, we interrogated a customized data set of genomic regions located within 10 kb of gene transcriptional start sites that are conserved in placental mammals with the GRHL3 consensus (and highly related sequences), an approach we had successfully employed to identify a key GRHL3 target in wound repair (Caddy et al., 2010). We identified a highly conserved site in the promoter region of the *Pten* gene (Figure 3A) (Li et al., 1997), and confirmed specific binding of GRHL3 to this site in vitro in electrophoretic mobility shift assays (EMSA) (Figure 3B), and in vivo by chromatin immunoprecipitation (ChIP) (Figure 3C). We also demonstrated that transcriptional activation of the *Pten* promoter by *Grhl3* was dependent on the integrity of this site in reporter gene assays (Figure S3A). Consistent with *Pten* being a direct target of GRHL3, expression of the gene was markedly reduced in the skin of *Grhl3* null E18.5 embryos at both RNA and protein level (Figure 3D).

Loss of *PTEN* leads to accumulation of PIP_3, and as a consequence, increased activity of the serine/threonine kinases PDK1 and AKT, with resultant activation of mTORC1 (Manning and Cantley, 2007). This leads to activation of S6K1 and phosphorylation of 4EBP1 and ribosomal protein S6, which provide a robust readout of mTORC1 signaling (Guertin and Sabatini, 2007; Ma and Blenis, 2009). Analysis of these downstream effectors of PI3K signaling in epidermis from *Grhl3* null embryos revealed increased levels of AKT, PDK1, S6, and 4EBP1, as well as their phosphorylated forms, p-AKT, p-PDK1, p-S6, and p-4EBP1

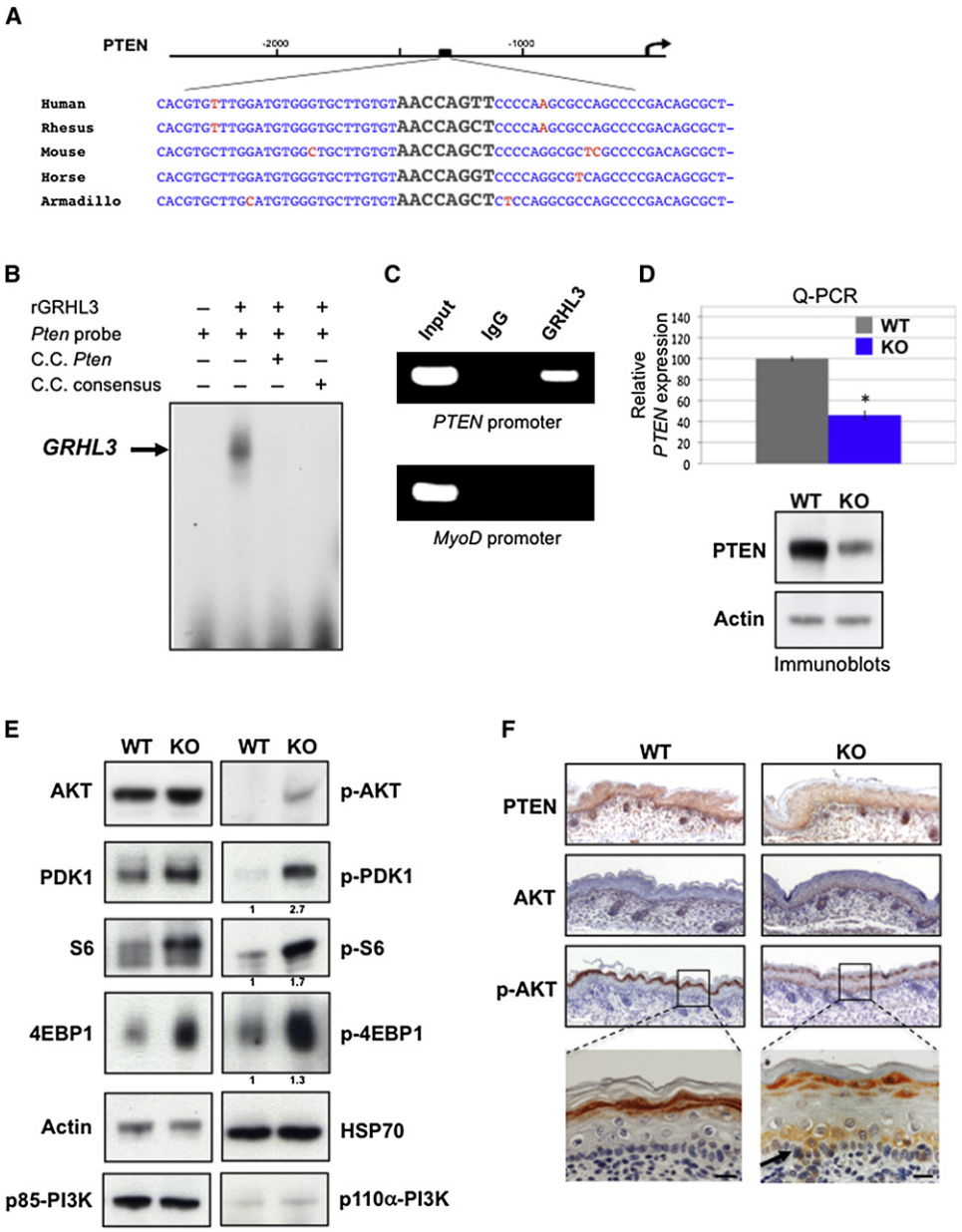

Figure 3. *PTEN* Is a Direct Transcriptional Target Gene of GRHL3

(A) Alignment of the promoter regions of *PTEN* genes from the indicated species. The GRHL3 DNA consensus sequence is enlarged and bolded. (See also Figure S3A.)

(B) EMSA of recombinant (r) GRHL3 binding to the *Pten* promoter probe. A 100-fold molar excess of unlabelled cold competitor probes (*Pten* or *Grhl3* consensus) was added in the indicated lanes. The migration of the specific GRHL3/DNA complex is arrowed.

(C) ChIP analysis of endogenous GRHL3 on the *PTEN* promoter. Chromatin from the human keratinocyte line (HaCaT) was immunoprecipitated using antisera to GRHL3, and amplified with *PTEN* primers. Preimmune sera (IgG) and the muscle-specific MyoD promoter were used as negative controls, and the input chromatin is shown.

(D) Q-RT-PCR (upper panel) and immunoblot (lower panel) of *Pten* expression in wild-type (WT) and *Grhl3*$^{-/-}$ (KO) E18.5 skin. For Q-RT-PCR, bars represent standard errors, and *HPRT* served as a reference. The difference in expression was statistically significant (*$p < 0.02$) using a Student's t test. For the immunoblot, actin served as the loading control. Error bars represent the standard deviation (±SD).

(E) Immunoblots of epidermal lysates from WT and KO E18.5 embryos probed with the stated antibodies. Actin and HSP70 served as loading controls. The fold induction of the phosphorylated proteins normalized to the levels of their nonphosphorylated counterparts is shown below each blot.

(F) IHC analysis of skin from WT and KO E18.5 embryos using the stated antibodies. Arrow in the lower right panel indicates p-AKT staining in the basal and adjacent suprabasal layers. Scale bars correspond to 200 μm (white) and 50 μm (black). (See also Figure S3B.)

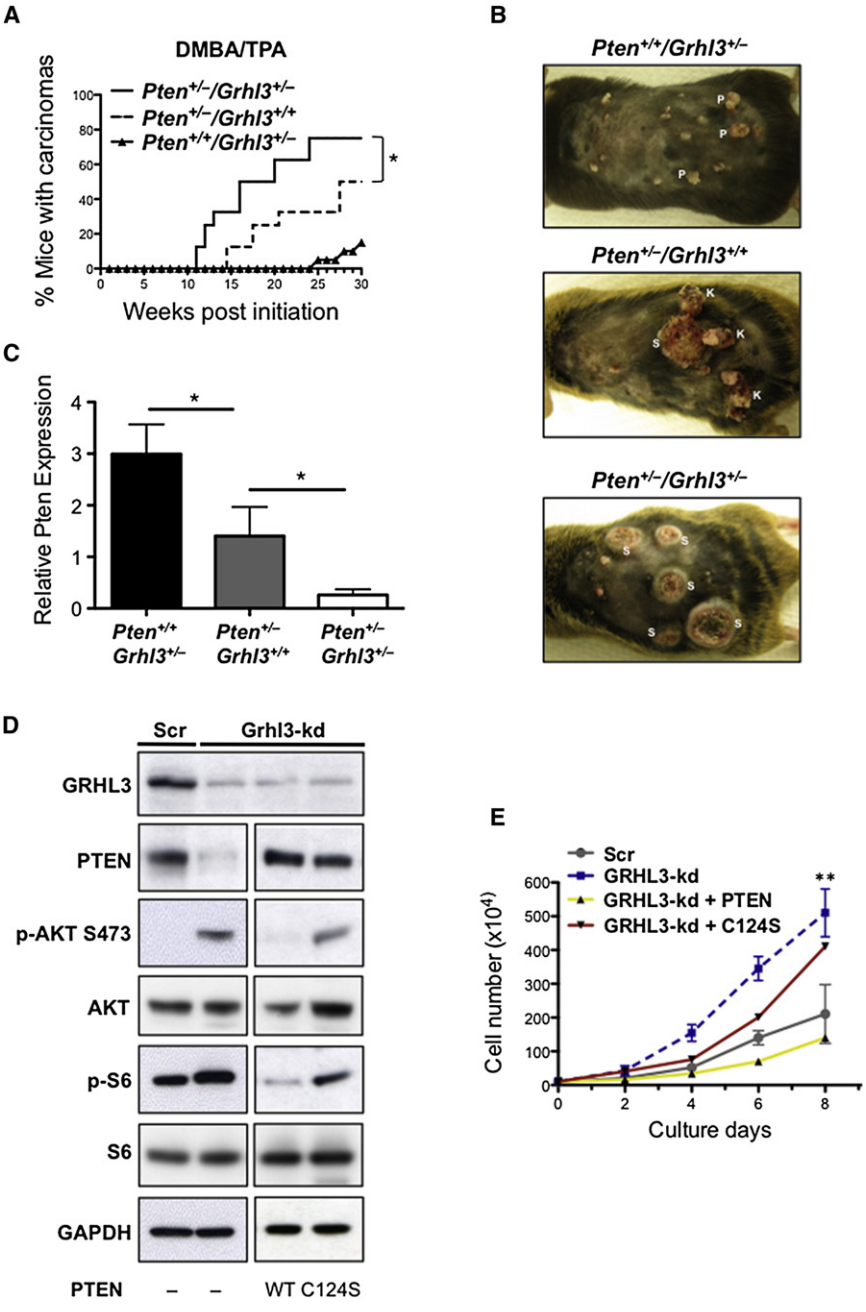

Figure 4. *Pten* Is the Critical GRHL3 Target Gene in Dysregulated Cell Growth and PI3K/AKT Activation

(A) Increased susceptibility of $Pten^{+/-}/Grhl3^{+/-}$ mice to DMBA/TPA-induced SCC. The difference in SCC incidence between $Pten^{+/-}/Grhl3^{+/-}$ and $Pten^{+/-}/Grhl3^{+/+}$ mice (*) was significant ($p < 0.05$) using the Student's t test.

(B) Macroscopic appearance of DMBA/TPA-treated $Pten^{+/+}/Grhl3^{+/-}$, $Pten^{+/-}/Grhl3^{+/+}$, and $Pten^{+/-}/Grhl3^{+/-}$ mice at 20 weeks. P, papilloma; K, kerato-acanthoma; S, SCC.

(C) *Pten* expression levels by Q-RT-PCR in normal skin from $Pten^{+/+}/Grhl3^{+/-}$, $Pten^{+/-}/Grhl3^{+/+}$, and $Pten^{+/-}/Grhl3^{+/-}$ mice. Error bars represent the standard deviation (±SD). The differences in Pten expression between the different lines (*) were statistically significant ($p < 0.05$) using a Student's t test.

(D) Immunoblots using the stated antibodies of lysates from GRHL3-kd and Scr HaCaT cells grown in serum, or transduced with MSCV-based retroviral supernatants carrying wild-type *PTEN* or the C124S phosphatase dead *PTEN* mutant as indicated. GAPDH served as the loading control. Error bars represent the standard deviation (±SD). (See also Figure S4A.)

(E) Growth kinetics of the cell lines listed in (D). A total of 1×10^5 cells for each line was seeded at day 0. The differences between the GRHL3-kd or GRHL3-kd + C124S mutant and the GRHL3-kd + wild-type *PTEN* or Scr cells at day 8 were significant ($p < 0.004$) using the Student's t test. Error bars represent the standard deviation (±SD).

(Figure 3E). This increase in abundance and activity of these proteins reflects a high level of mTORC1 signaling (Ma and Blenis, 2009). The levels of the catalytic p110α isoform and the p85 regulatory subunit of the PI3K protein, which lie upstream of PTEN, were not altered. PTEN levels were markedly reduced in the basal layer of the epidermis, and coincident with this, the levels of p-AKT were increased in this layer, and the adjacent suprabasal layer (Figure 3F). The size of the cells in the basal layer was also increased (Figure S3B), a feature common to cells from mice lacking *Pten* (Groszer et al., 2001).

To determine whether *Grhl3* and *Pten* interacted epistatically, we intercrossed mice carrying heterozygous deletions of the two genes to generate compound heterozygotes ($Grhl3^{+/-}/Pten^{+/-}$), and compared these animals with $Grhl3^{+/-}/Pten^{+/+}$ and $Grhl3^{+/+}/Pten^{+/-}$ controls in the chemical-induced tumor model (n = 10 in each group) (Figure 4A). Although mice heterozygous for *Pten* alone ($Grhl3^{+/+}/Pten^{+/-}$) display increased susceptibility to DMBA/TPA-induced tumors (Mao et al., 2004), the additional loss of a single *Grhl3* allele enhanced both the rapidity of cancer development and the number of mice with multiple aggressive SCCs (Figure 4B). Conversely, the restoration of *Pten* to wild-type status in the $Grhl3^{+/-}/Pten^{+/+}$ mice almost completely safeguarded these animals against SCC formation. The susceptibility of the different genotypes to SCC was reflected in their levels of *Pten* expression (Figure 4C). Taken together, these data suggest that *Pten* is the critical downstream target of *Grhl3* for prevention of SCC. To confirm this in a human model, we generated a human keratinocyte cell line (HaCaT) in which the expression of GRHL3 had been knocked down using a specific shRNA containing lentivirus (GRHL3-kd) (Figure 4D) (Caddy et al., 2010). A line transduced with a scrambled control (Scr) shRNA served as the control. In keeping with our earlier findings, the level of PTEN was markedly reduced in the

GRHL3-kd line compared to control, and p-AKT and p-S6 levels were increased in these cells in both the presence (Figure 4D) and absence of serum (Figure S4). This latter result was consistent with the resistance to growth factor and nutrient withdrawal observed with constitutive PI3K activation in tumor cell lines (Kalaany and Sabatini, 2009). The GRHL3-kd cells also proliferated more rapidly than the Scr cells (Figure 4E). Reintroduction of wild-type PTEN into the GRHL3-kd line restored the inhibition of phosphorylation of AKT and S6 (Figure 4D), and led to suppression of cell growth (Figure 4E). In contrast, introduction of the C124S phosphatase dead PTEN mutant (Myers et al., 1998), to equivalent levels to that achieved with the wild-type protein, failed to inhibit AKT and S6 phosphorylation (Figure 4D), and also failed to suppress the enhanced proliferation of the GRHL3-kd cells (Figure 4E). These findings suggest that *Pten* is the critical downstream target of GRHL3 in tumorigenesis.

Activation of PI3K/AKT and Repression of Ras/MAPK/ERK Signaling in *Grhl3*-Deficient Tumors

We next compared PTEN levels and PI3K signaling in unaffected skin, papillomas, and SCCs derived from both wild-type and *Grhl3*$^{\Delta/-}$/*K14Cre*+ mice (Figures 5A and 5B). Cellular proliferation in the SCCs was demonstrated by PCNA staining (Figure S5A). Loss of GRHL3 was associated with a reduction in PTEN in unaffected skin, and almost complete loss in papillomas and SCCs that was not observed in the wild-type skin or tumors. This was accompanied by increased levels of p-S6 and p-AKT in the tumors from *Grhl3*$^{\Delta/-}$/*K14Cre*+ mice. Although p-S6 levels were also increased in the tumors from wild-type mice, p-AKT expression was weak, suggesting that the increase in p-S6 was due to other pathways feeding into the mTORC1 pathway below the level of AKT (Carracedo and Pandolfi, 2008). Of note the increase in p-AKT in the SCC from *Grhl3*$^{\Delta/-}$/*K14Cre*+ mice compared to wild-type controls was due to both the number of positively staining cells in the tumors and the staining intensity (Figures S5B and S5C).

Previous studies have suggested that activation of *H-ras* and complete loss of *Pten* are mutually exclusive in skin carcinomas (Mao et al., 2004). Our findings confirmed this because we detected no mutations in codons 12, 13, or 61 in the *H-Ras* gene in tumors derived from *Grhl3*$^{\Delta/-}$/*K14Cre*+ mice, whereas 16% of tumors from the wild-type mice carried mutations in these codons (Figure 5C). Similar frequencies of *H-Ras* mutations have been detected in series of human SCC (Boukamp, 2005). We also observed an almost complete absence of p-ERK1/2 in tumors from the *Grhl3*$^{\Delta/-}$/*K14Cre*+ mice despite levels of ERK1/2 that were comparable to unaffected skin, and skin from wild-type controls (Figures 5D and 5E). This finding was comparable to the reduction in p-ERK1/2 that we had previously described in the epidermis of *Grhl3* null embryos (Hislop et al., 2008). In contrast the levels of p-ERK1/2 in tumors from wild-type mice were markedly elevated (Figures 5D and 5E).

A miR-21-Dependent Proto-Oncogene Network Targets GRHL3 and PTEN

To establish the relevance of our mouse findings in the human system, we analyzed the expression of *GRHL3* by Q-RT-PCR in 37 consecutive primary human SCCs, and the adjacent nontumor-affected epidermis isolated by laser capture microdissection (LCM). In almost all cases *GRHL3* levels were markedly reduced in the tumors compared to the adjacent epidermis, with expression reduced by more than 90% in over half the samples (Figure 6A). A coordinate reduction in *PTEN* expression was also observed in these tumors (Figure 6A ; Figure S6A). Interestingly, a similar reduction in *GRHL3* and *PTEN* levels was also observed in SCCs of head and neck origin (HNSCCs) (Figure S6B), suggesting a common molecular mechanism for cancers of this histological subtype. Sequence analysis of the *GRHL3* coding exons and splice donor and acceptor sites failed to detect any mutations in the tumors, and the methylation status of the CpG islands in the GRHL3 promoter was unchanged in tumors compared to normal skin (data not shown).

An alternate mechanism for the reduction in *GRHL3* expression in the tumors could be through overexpression of a specific microRNA (miRNA), which have been shown in some contexts to function as oncogenes by targeting tumor suppressors (Hammond, 2006; Esquela-Kerscher and Slack, 2006; Garzon et al., 2010). To examine this, we interrogated a miRNA array with total RNA derived from two human SCCs with undetectable levels of *GRHL3*, and their matched normal skin controls (Figure 6B). We focused on miRNAs that were predicted to target *GRHL3* using the mirWIP database (Hammell et al., 2008). Of this set, miR-21 exhibited the greatest differential between normal and tumor tissue, and its sequence aligned with nucleotides 414–436 in the *GRHL3* 3′UTR (Figure 6C). Interestingly, miR-21 has previously been shown to function as an oncogene by targeting *PTEN* (Meng et al., 2007). We examined an additional ten SCCs, and their matched controls, and demonstrated a greater than 6-fold difference in miR-21 expression between the two groups (Figure 6D). We confirmed that enforced expression of miR-21 (Figure S6C) could inhibit *GRHL3* mRNA expression in the human HaCaT cell line (Figure 6E), in keeping with recent reports indicating that mRNA destabilization usually comprised the major component of miR-dependent gene repression (Baek et al., 2008; Selbach et al., 2008). Expression of *PTEN* mRNA was also reduced in this line, consistent with the effect on *GRHL3*, and with direct targeting of *PTEN* by miR-21 (Figure 6F). GRHL3 and PTEN protein levels were also markedly reduced in the miR-21 expressing HaCaT cells (Figure 6G), and this was accompanied by enhanced cell growth (Figure S6D). We established that *GRHL3* was a direct target of miR-21, using a luciferase reporter linked to the *GRHL3* 3′UTR (Figure 6H). Cotransfection of this construct with a miR-21 expression vector into HEK293 cells resulted in a marked reduction in luciferase activity compared to a Scr sequence, and this was reversed when an antagomir of miR-21 (miRZip21) was also transfected. Deletion of the miR-21 binding site in the *GRHL3* 3′UTR completely abrogated its effect (Figure 6H), indicating that *GRHL3* is a direct target of miR-21.

The miR-21-Dependent Proto-Oncogene Network Is Active in Both Skin and HNSCC

To determine whether the miR-21-dependent proto-oncogene network had broader relevance in SCC, we examined expression of miR-21, *GRHL3*, and *PTEN* in a range of human SCC cell lines derived from both epidermal (SCC-13), and head and neck (SCC-4, -9, -15, -25, and CAL-27) origins. All SCC lines tested, except SCC-4, exhibited elevated levels of miR-21

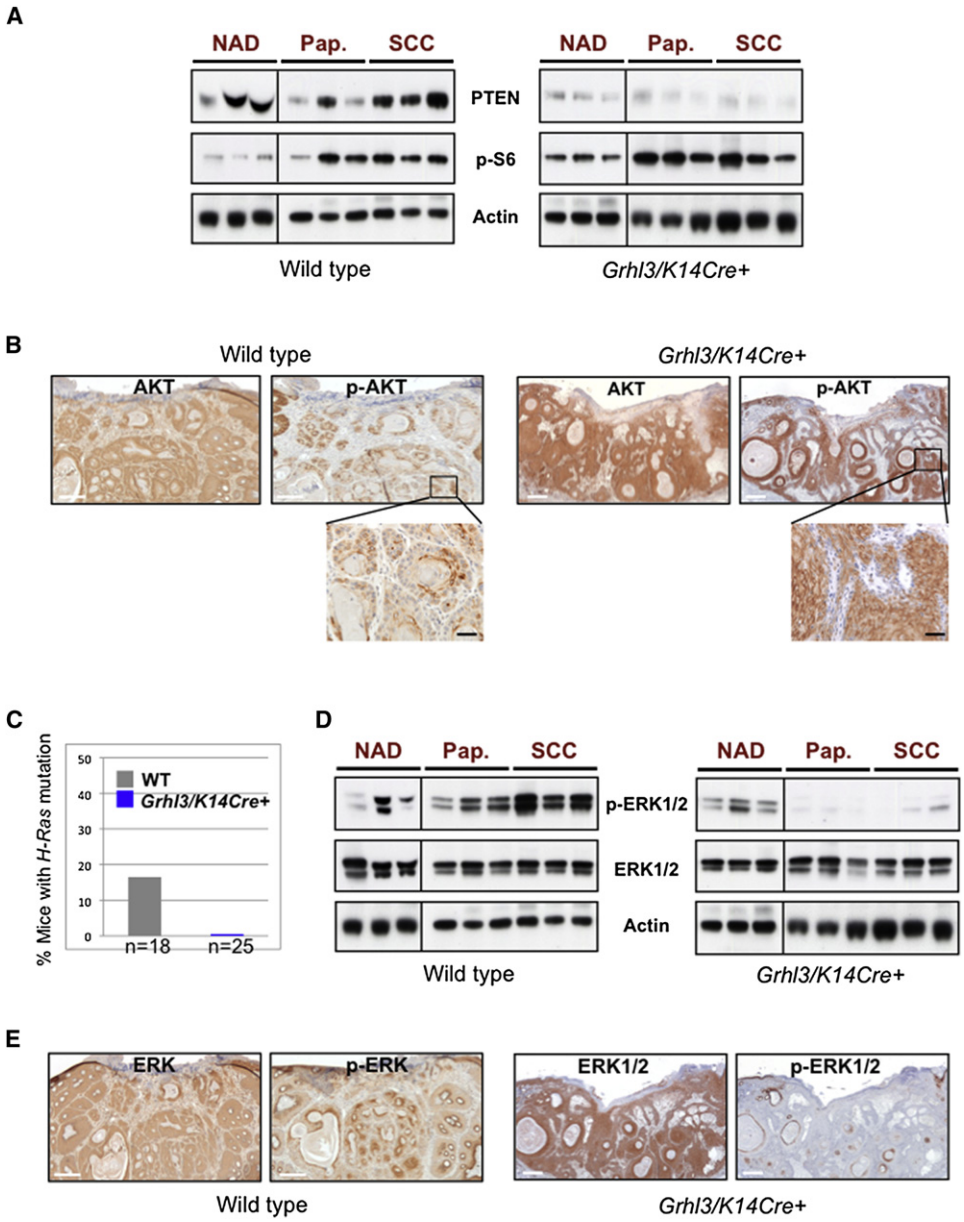

Figure 5. Skin and Tumors from *Grhl3*$^{\Delta/-}$/*K14Cre*+ Mice Exhibit PI3K Pathway Activation

(A) Immunoblot of lysates from epidermis (NAD), papillomas (Pap.), and SCCs from wild-type and *Grhl3*$^{\Delta/-}$/*K14Cre*+ mice probed with PTEN and p-S6 antibodies. Actin served as the loading control.

(B) IHC analysis of SCC from wild-type and *Grhl3*$^{\Delta/-}$/*K14Cre*+ mice using AKT and p-AKT antibodies. (See also Figures S5A–S5C.)

(C) Analysis of *H-Ras* mutations in tumors from wild-type and *Grhl3*$^{\Delta/-}$/*K14Cre*+ mice.

(D) Immunoblot of lysates from epidermis, papillomas, and SCCs from wild-type and *Grhl3*$^{\Delta/-}$/*K14Cre*+ mice probed with ERK1/2 and p-ERK1/2 antibodies. The actin loading control is shown and is the same as for (A).

(E) IHC analysis of SCC from wild-type and *Grhl3*$^{\Delta/-}$/*K14Cre*+ mice using ERK1/2 and p-ERK1/2 antibodies.

Scale bars correspond to 200 μm (white) and 50 μm (black).

compared to HaCaT cells, with corresponding reductions in both *GRHL3* and *PTEN* levels (Figure 7A). To assess the consequences of inhibition of miR-21 in HNSCC, we utilized the miRZip21 antagomir in the SCC-9 cell line, achieving a substantial reduction in miR-21 levels compared to cells transduced with a Scr control (Figure 7B). This resulted in a greater than 10-fold induction of *GRHL3* expression at both RNA (Figure 7C) and protein (Figure 7D) level, resulting in increased levels of PTEN, inhibition of PI3/AKT signaling (Figure 7D), and marked inhibition of cell proliferation (Figure 7E). These finding suggest that activation of the miR-21-dependent proto-oncogene network may be a common molecular mechanism in SCC of different tissue origins, and that targeting of this network may have therapeutic potential.

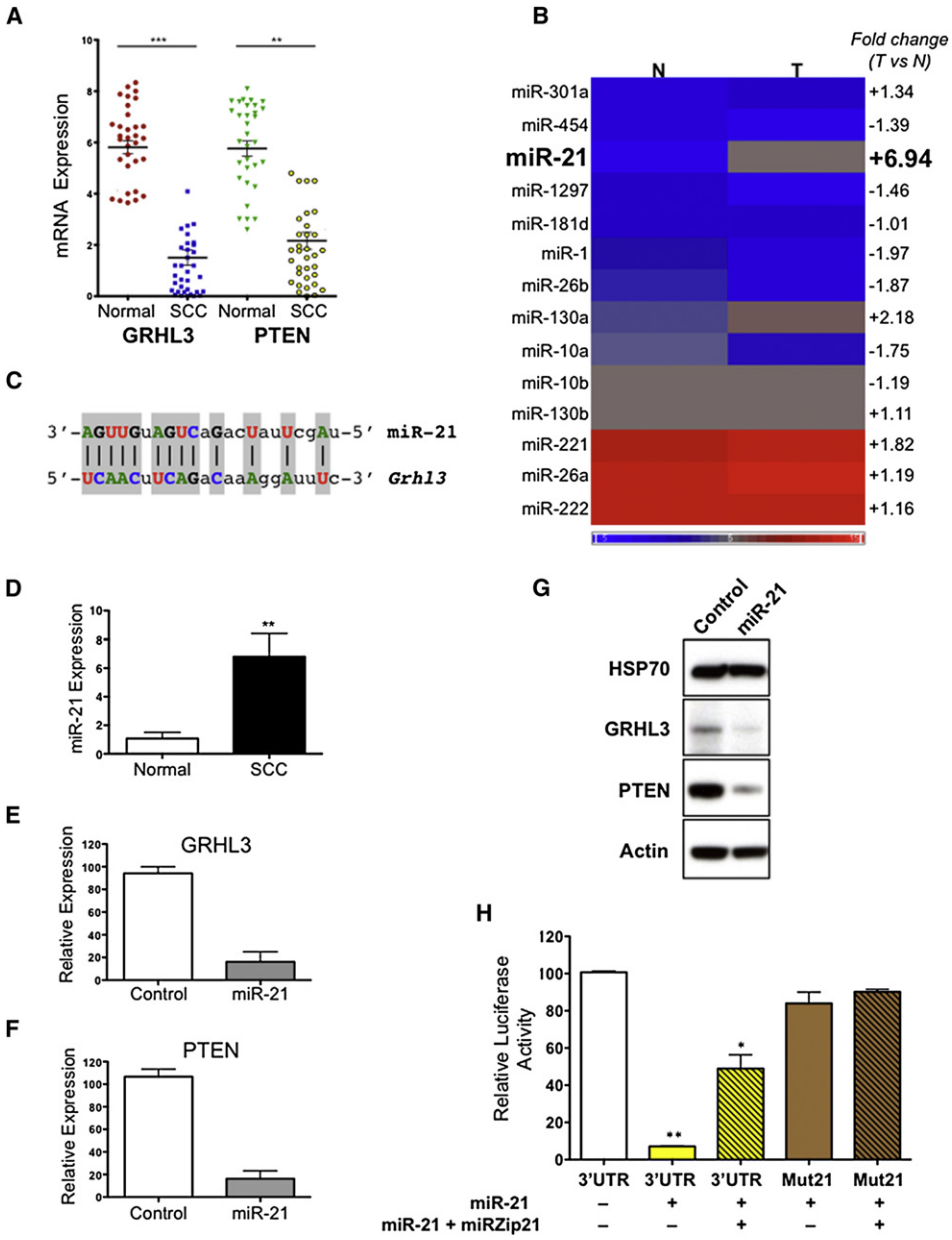

Figure 6. miR-21-Induced Loss of *GRHL3* and *PTEN* Expression in Human SCC

(A) Quantification of *GRHL3* and *PTEN* expression levels by Q-RT-PCR in human SCCs isolated by LCM, normalized to expression in the adjacent nontumor-containing tissue. The differences in GRHL3 (***) and PTEN (**) expression between normal tissues and SCCs were statistically significant ($p < 0.02$ and $p < 0.05$, respectively) using a Student's t test. Error bars represent ±SEM. (See also Figures S6A and S6B.)

(B) Heat map of the relative expression of miRNAs predicted to target *GRHL3* in two human SCCs and the adjacent normal epidermis. The fold change in tumor (T) versus normal (N) is shown.

(C) Alignment between miR-21 and the 3′UTR of human *GRHL3*.

(D) Quantification of human miR-21 expression levels relative to U6 by Q-RT-PCR in ten SCCs and their matched controls. The difference in miR-21 expression (**) between normal tissues and SCCs was statistically significant ($p < 0.02$) using a Student's t test. Error bars represent the standard deviation (±SD).

(E) *GRHL3* and (F) *PTEN* expression quantitated by Q-RT-PCR and normalized to β-actin in HaCaT cells overexpressing miR-21 or a Scr control. Error bars represent the standard deviation (±SD).

(G) Immunoblots of lysates from control and miR-21 overexpressing HaCaT cells probed with the stated antibodies. Actin and HSP70 served as the loading controls. (See also Figures S6C and S6D.)

(H) Luciferase activity of the wild-type (3′UTR) or mutant (Mut21) *GRHL3* 3′UTR reporter constructs transfected into HEK293 cells in the presence and absence of expression vectors carrying miR-21 or its antagomir (miRZip21) as indicated. Expression of β-galactosidase from a cotransfected reporter construct was used as control for transfection efficiency. The differences in relative luciferase activity between the GRHL3 3′UTR construct transfected alone, or cotransfected with miR-21 alone (**), or miR-21 and miRZip21 (*) were statistically significant ($p < 0.01$ and $p < 0.05$, respectively) using a Student's t test. Error bars represent the standard deviation (±SD).

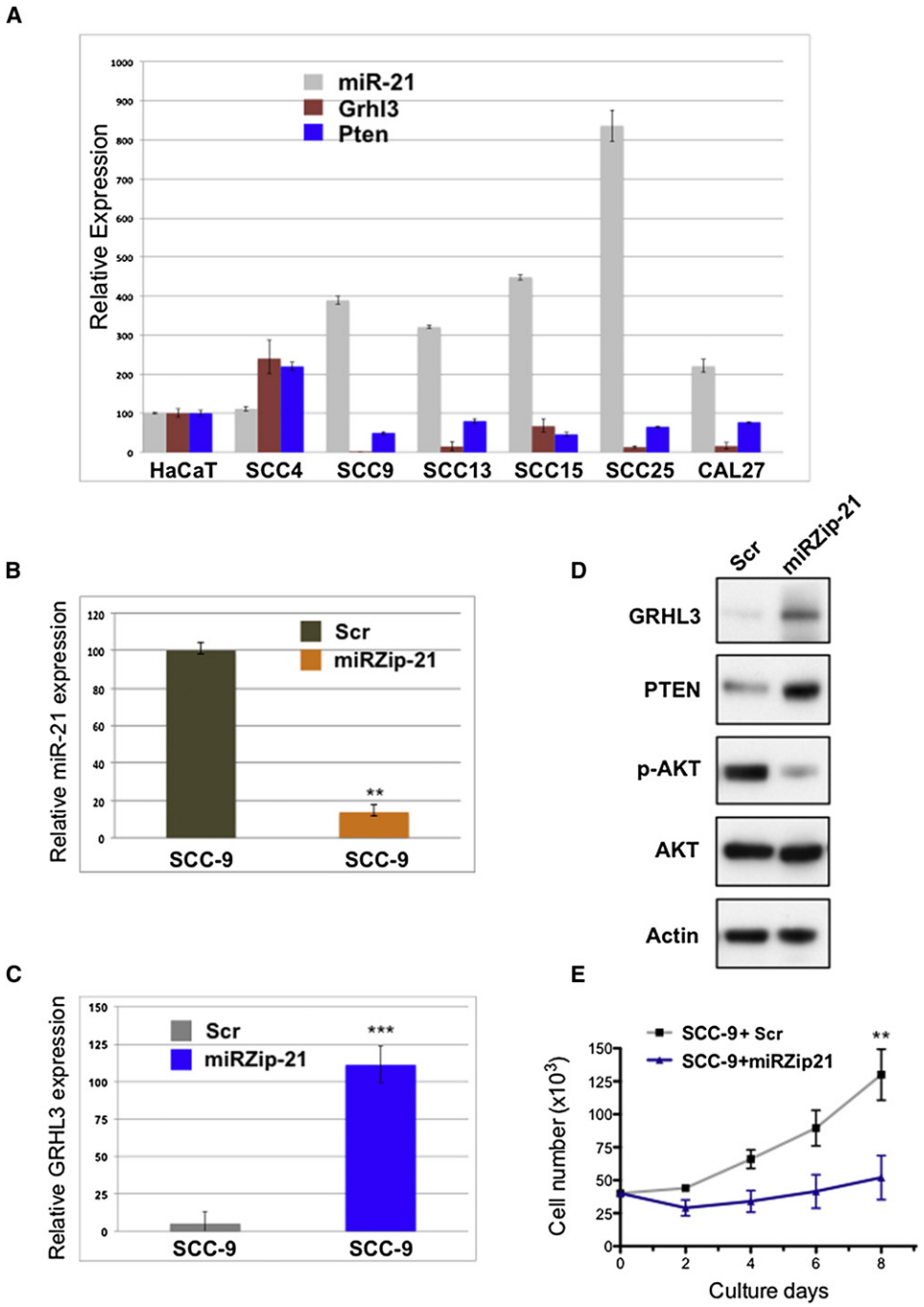

Figure 7. The miR-21-Dependent Proto-Oncogene Network Is Active in Both Skin and HNSCC Cell Lines

(A) miR-21, *GRHL3*, and *PTEN* expression levels in SCC cell lines relative to HaCaT cells.

(B) Quantification of miR-21 expression by Q-PCR in SCC-9 cells transinfected with the lentiviral vector-based miR-21 antagomir (miRZip21) or a Scr control. The difference in expression (**) was statistically significant ($p < 0.005$) using a Student's t test.

(C) Quantification of *GRHL3* expression by Q-PCR in SCC-9 cells transinfected with the lentiviral vector-based miR-21 antagomir (miRZip21) or a Scr control. The difference in expression (***) was statistically significant ($p < 0.002$) using a Student's t test.

(D) Immunoblots using the stated antibodies of lysates from SCC-9 cells transduced with a lentivirus carrying the miRZip-21 or Scr control. Actin served as the loading control.

(E) Growth kinetics of the cell lines listed in (D). A total of 4×10^4 cells for each line was seeded at day 0. The differences between the SCC-9 + miRZip-21 and SCC-9 + Scr cells at day 8 were significant (**) ($p < 0.003$) using the Student's t test.

Error bars represent the standard deviation (±SD) in (A)–(C) and (E).

DISCUSSION

Our data define the *Grhl3* gene as a potent suppressor of SCC of the skin in mammals, acting through the direct transcriptional regulation of *Pten*. Supporting this conclusion are phylogenetic, biochemical, and expression data coupled with functional rescue studies in vitro in a human system, and in vivo in the mouse. In addition, clear parallels exist between *Grhl3*-deficient mice and mice lacking *Pten* in the adult epidermis, although the phenotype in the latter animals is somewhat variable, and is dependent on the strategy utilized for gene deletion (Suzuki et al., 2003; Yao et al., 2006; Mao et al., 2004). Our findings also implicate *Grhl3* in the pathogenesis of HNSCC in humans, providing possible alternate therapeutic strategies for targeting cancers that are often associated with an extremely poor prognosis.

Although *PTEN* has been thought to be constitutively expressed, and minimally regulated in normal tissues (Salmena et al., 2008), our findings refute this paradigm in one setting by establishing the pivotal importance of tissue-specific control of *Pten* expression in suppression of SCC. The integral function of *Grhl3* in this process, coupled with its role in maintaining the balance between keratinocyte differentiation and proliferation, defines *Grhl3* as a critical innate surveillant to prevent skin cancer. In this regard its function is similar to IKKα, which also induces keratinocyte terminal differentiation and prevents SCC (Liu et al., 2008; Park et al., 2007). However, in contrast to IKKα-deficient tumors that exhibit EGFR-induced ERK activation, loss of *Grhl3* results in exclusive upregulation of PI3K/AKT/mTOR signaling, with a complete loss of p-ERK expression and no change in the levels of p-EGFR (Figure S3C). The absence of *Ras* mutations and the marked downregulation of the MAPK/ERK-signaling pathway in the tumors from *Grhl3*$^{\Delta/-}$/*K14Cre*+ mice are similar to the findings observed in *Pten*-deficient mice (Mao et al., 2004), indicating that in the absence of *Pten*, this pathway is dispensable for SCC formation. Similar results were also observed in RU486-inducible *K14.Cre/Pten*$^{fl/fl}$ mice that coexpress an *Ha-Ras* transgene, in which TPA-mediated tumor progression involved PTEN-associated pathways rather than Ras activation (Yao et al., 2006).

Although we have now identified several GRHL3 target genes that are involved in the diverse developmental processes regulated by this transcription factor (Caddy et al., 2010; Ting et al., 2005), the loss of *Pten* alone appears to be sufficient for the increased susceptibility of the *Grhl3*-deficient mice to both chemical-induced and spontaneous SCC. This is illustrated by the profound difference in cancer susceptibility between *Grhl3*$^{+/-}$/*Pten*$^{+/+}$ mice (that develop no tumors) and *Grhl3*$^{+/-}$/*Pten*$^{+/-}$ animals (that display multiple aggressive SCC)—with these two lines differing only by the addition of a single functional *Pten* allele. A substantial difference in SCC susceptibility was also observed between *Grhl3*$^{+/+}$/*Pten*$^{+/-}$ mice and the compound heterozygotes, consistent with recent data showing that subtle differences in *Pten* expression levels can have profound consequences on cancer susceptibility (Alimonti et al., 2010). Our data in GRHL3-kd keratinocytes also indicate that *PTEN* is the critical downstream target of *GRHL3* in the human system, with wild-type, but not a phosphatase-dead mutant PTEN, able to repress PI3K/AKT/mTOR signaling and inhibit cell hyperproliferation. This is further supported by our studies on the SCC9 cell line, in which miRZip21-induced enhanced expression of GRHL3 leads to upregulation of PTEN levels, suppression of PI3K/AKT signaling, and reduced cell proliferation.

The reduced expression of both *GRHL3* and *PTEN* mediated by upregulation of miR-21 in human skin SCC explains the long-standing paradox of loss of PTEN expression in the absence of genetic or epigenetic alterations to the gene (Ming and He, 2009). The coordinate targeting of both tumor suppressors by miR-21 provides a classic example of the emerging theme of miRNA-dependent amplification of signaling cascades, which are evident in both normal and cancerous tissues (Inui et al., 2010). In this setting the synchronous regulation of the pathway inhibitor (*PTEN*) and its transcriptional regulator (*GRHL3*) by a solitary miR (miR-21) establishes a proto-oncogenic network involving enhanced PI3K/AKT/mTOR signaling in these tumors. The extension of our findings from skin SCC to HNSCC is in keeping with the common embryonic origins of these tissues, and the expression of *Grhl3* in all adult epithelium derived from the developing surface ectoderm. It is also consistent with previous studies identifying *GRHL3* as a gene exhibiting reduced expression in primary and metastatic HNSCC (Nguyen et al., 2007; Rickman et al., 2008), and with the increased expression of miR-21 reported in multiple HNSCC series (Volinia et al., 2006; Avissar et al., 2009; Hui et al., 2010).

Emerging from our work is an increased rationale for the use of direct inhibitors of PI3K/AKT/mTORC1 signaling and/or antagonists of miR-21 in the treatment of SCC. Recent studies have identified an mTORC1-PI3K-dependent negative feedback loop regulating MAPK/ERK signaling in cancer, with increased p-ERK levels observed in tumors treated with the TORC1 inhibitor RAD001 (Carracedo et al., 2008). It will be of considerable interest to determine whether *Grhl3*-dependent skin SCCs display activation of MAPK/ERK signaling when treated with TORC1 inhibitors, or alternatively, exhibit true oncogene addiction to constitutively active PI3K/AKT/mTOR signaling. The latter finding may pave the way for novel therapeutic interventions in invasive SCC of the skin. In the context of HNSCC, new treatments have focused on inhibitors of EGFR, although targeting of the PI3K/AKT pathway is also under investigation (Leemans et al., 2011). As with other cancers, the PTEN expression status may influence response to EGFR inhibitors (Jhawer et al., 2008), and antagonists of miR-21 may offer benefits as single agents, or in combination with agents such as cetuximab.

EXPERIMENTAL PROCEDURES

Generation of Experimental Animals

All experiments were preapproved by The University of Melbourne Animal Ethics Committee. The generation and genotyping of *Grhl3*$^{+/-}$ mice have been described previously (Ting et al., 2003). The conditional *Grhl3* targeting vector was constructed and validated as detailed in the Supplemental Experimental Procedures (Figures S1A–S1C). *Grhl3*$^{+/-}$ mice were crossed with *K14Cre*+ transgenic mice (Jonkers et al., 2001), and the resultant animals were crossed with *Grhl3*$^{fl/fl}$ mice to provide the *Grhl3*$^{\Delta/-}$/*K14Cre*+ experimental animals (where Δ is the deleted *floxed* allele). *Pten*$^{+/-}$ mice were kindly provided by Dr. Tak Mak, and intercrossed with *Grhl3*$^{+/-}$ mice to generate compound heterozygotes.

Tumor Induction and Skin Barrier Analysis in Mice

Tumors were induced in mice through the application of 25 μg DMBA (Sigma-Aldrich) in acetone to a shaved area on the back followed 1 week later by

twice-weekly application of TPA (7.6 nmol) in 150 μl of acetone for up to 30 weeks. In some experiments TPA was applied without DMBA initiation. Skin barrier analysis was performed as previously described (Hardman et al., 1998).

RNA Preparation and Q-RT-PCR

For gene expression analysis, normal skin from E18.5 wild-type and *Grhl3*$^{-/-}$ embryos, and adult wild-type and *Grhl3*$^{\Delta/-}$/*K14Cre*+ mice, and papillomas and SCC from wild-type and *Grhl3*$^{\Delta/-}$/*K14Cre*+ mice were homogenized in TRIzol (Invitrogen) and RNA extracted according to the manufacturer's instructions. Q-RT-PCR was carried out as described previously (Ting et al., 2003) with primer sequences shown in the Supplemental Experimental Procedures. A Student's t test was used to determine statistical difference in expression levels with p values <0.05 considered significant, and results were analyzed using Prism (GraphPad). The error bars in all expression analyses represent the standard error of the mean (SEM).

ChIP and EMSA

ChIP was performed as described previously (Wilanowski et al., 2008), with anti-GRHL3 antibodies (Aviva Systems Biology, San Diego, CA). EMSAs were performed using recombinant mouse GRHL3 protein, and oligonucleotides containing the conserved GRHL3-binding site in the *Pten* promoter. The DNA consensus-binding site for GRHL3 was used as a cold competitor (Ting et al., 2005). Primer and oligonucleotide sequences for the *Pten* promoter are shown in the Supplemental Experimental Procedures.

Immunoblot Analysis and IHC

Immunoblotting and IHC methodologies and the antibodies employed are detailed in the Supplemental Experimental Procedures. For quantification of IHC, eight images (20×) were taken per tumor and the positive p-AKT cells counted. The staining intensity of the tumor was quantified using MetaMorph image analysis software and plotted as percentage of staining intensity of the total area (Hambardzumyan et al., 2008).

shRNAs and Retroviral Infection

The shRNA target oligonucleotides for *Grhl3* and the Scr were cloned into the pSUPER.retro.neo+GFP vector using the BglII and HindIII sites. The target sequences and generation of viruses are detailed as previously described (Caddy et al., 2010). HaCaT cells were transduced over a 24 hr period, and GFP-positive cells were selected by FACS, and cultured for 8 days, or harvested for preparation of lysates. Knockdown of GRHL3 expression was confirmed by immunoblot using antibodies to GRHL3 and GAPDH. For expression of wild-type *PTEN*, or the phosphatase dead C124S *PTEN* mutant in GRHL3-kd cells, the respective cDNAs were cloned into MSCV-DSRed using the BamHI and XhoI sites. PTEN expression was confirmed in DSRed+ cells by immunoblot using PTEN antibody, and GAPDH as a loading control.

LCM

Deidentified surgical specimens of SCC resected from patients (including tumor and adjacent normal tissue) were embedded in OCT medium and stored at −80°C. The sections were stained with HistoGene LCM Frozen Staining Kit just before commencing LCM. The cryosections (8 μm) were microdissected using a Veritas™ microdissection instrument (Arcturus) according to the standard protocol. Tumor tissues and normal tissues were captured onto CapSure Macro LCM Caps. RNA extraction and amplification were performed according to the manufacturer's instructions. The reagents for staining, RNA extraction, and RNA amplification were obtained from Arcturus. Q-RT-PCR was performed as detailed above. Ethics approvals were obtained from the Victorian Tissue Biobank and the Human Research Ethics Committee of the Royal Melbourne Hospital.

Mutational Analysis of *H-ras*

PCR primers amplifying codons 12, 13, and 61 were designed on the basis of genomic DNA sequences for *H-ras*. Mutations were detected by sequencing as previously described (Ise et al., 2000). The mutations were further confirmed by restriction fragment length polymorphism (RFLP) analysis as previously detailed (Jaworski et al., 2005).

Luciferase Assays

Reporter gene analysis of the *Pten* promoter is detailed in the Supplemental Experimental Procedures. For analysis of miR-21 regulation of *GRHL3*, the 3′UTR region of human *GRHL3* containing the predicted site for miR-21 was subcloned into the pMIR-REPORT luciferase vector (pMIR-*GRHL3′UTR* luciferase) (Applied Biosystems). A mutant construct (Mut21) was generated by deleting 10 bp (419–428) from the miR-21 site in the 3′UTR of *GRHL3* (pMIR-*GRHL3′UTR-Mut21* luciferase). Both constructs (0.5 μg) were transfected into HEK293T cells with the pMIR-β-galactosidase vector. After 15 hr, the miR-21 precursor construct was coinfected with and without the lentivector-based antagomir to miR-21 "miRZip-21" (System Biosciences). Firefly luciferase was measured 48 hr after transfection/infection using the Dual-Light Chemiluminescent Reporter Gene Assay System (Applied Biosystems), as per the manufacturer's instructions, and normalized to β-galactosidase activity to control for differences in transfection efficiency.

ACCESSION NUMBERS

The data set for the GeneChip miRNA Array has been deposited in the Gene Expression Omnibus database with accession code GSE32868.

SUPPLEMENTAL INFORMATION

Supplemental Information includes six figures and Supplemental Experimental Procedures and can be found with this article online at doi:10.1016/j.ccr.2011.10.014.

ACKNOWLEDGMENTS

We thank Andreas Strasser, George Thomas, and Paul Mischel for critical appraisal of the manuscript; the staff from the Bio21 Institute for animal care; the Victorian Cancer Biobank for human SCC samples; Dr. Hong-Jian Zhu for constructs; Dr. Tak Mak for *Pten*$^{+/-}$ mice; Dr. Garry Anderson for assistance with biostatistical analysis; Dr. Michael Buchert for assistance with IHC quantification; and the Australian Cancer Research Foundation for the LCM. S.M.J. is a Principal Research Fellow of the Australian National Health and Medical Research Council (NHMRC). The work was partially supported by Project Grants from the NHMRC, and Grants from the Association for International Cancer Research and the March of Dimes Foundation.

Received: April 19, 2011
Revised: September 2, 2011
Accepted: October 13, 2011
Published: November 14, 2011

REFERENCES

Abel, E.L., Angel, J.M., Kiguchi, K., and DiGiovanni, J. (2009). Multi-stage chemical carcinogenesis in mouse skin: fundamentals and applications. Nat. Protoc. *4*, 1350–1362.

Alam, M., and Ratner, D. (2001). Cutaneous squamous-cell carcinoma. N. Engl. J. Med. *344*, 975–983.

Alimonti, A., Carracedo, A., Clohessy, J.G., Trotman, L.C., Nardella, C., Egia, A., Salmena, L., Sampieri, K., Haveman, W.J., Brogi, E., et al. (2010). Subtle variations in Pten dose determine cancer susceptibility. Nat. Genet. *42*, 454–458.

Avissar, M., Christensen, B.C., Kelsey, K.T., and Marsit, C.J. (2009). MicroRNA expression ratio is predictive of head and neck squamous cell carcinoma. Clin. Cancer Res. *15*, 2850–2855.

Baek, D., Villén, J., Shin, C., Camargo, F.D., Gygi, S.P., and Bartel, D.P. (2008). The impact of microRNAs on protein output. Nature *455*, 64–71.

Bos, J.L. (1989). ras oncogenes in human cancer: a review. Cancer Res. *49*, 4682–4689.

Boukamp, P. (2005). Non-melanoma skin cancer: what drives tumor development and progression? Carcinogenesis *26*, 1657–1667.

Bray, S.J., and Kafatos, F.C. (1991). Developmental function of Elf-1: an essential transcription factor during embryogenesis in *Drosophila*. Genes Dev. *5*, 1672–1683.

Caddy, J., Wilanowski, T., Darido, C., Dworkin, S., Ting, S.B., Zhao, Q., Rank, G., Auden, A., Srivastava, S., Papenfuss, T.A., et al. (2010). Epidermal wound repair is regulated by the planar cell polarity signaling pathway. Dev. Cell *19*, 138–147, Erratum: (2010). Dev. Cell *19*, 353.

Carracedo, A., and Pandolfi, P.P. (2008). The PTEN-PI3K pathway: of feedbacks and cross-talks. Oncogene *27*, 5527–5541.

Carracedo, A., Ma, L., Teruya-Feldstein, J., Rojo, F., Salmena, L., Alimonti, A., Egia, A., Sasaki, A.T., Thomas, G., Kozma, S.C., et al. (2008). Inhibition of mTORC1 leads to MAPK pathway activation through a PI3K-dependent feedback loop in human cancer. J. Clin. Invest. *118*, 3065–3074.

Clayton, E., Doupé, D.P., Klein, A.M., Winton, D.J., Simons, B.D., and Jones, P.H. (2007). A single type of progenitor cell maintains normal epidermis. Nature *446*, 185–189.

Dajee, M., Lazarov, M., Zhang, J.Y., Cai, T., Green, C.L., Russell, A.J., Marinkovich, M.P., Tao, S., Lin, Q., Kubo, Y., and Khavari, P.A. (2003). NF-kappaB blockade and oncogenic Ras trigger invasive human epidermal neoplasia. Nature *421*, 639–643.

Dean, M. (1998). Cancer as a complex developmental disorder—nineteenth Cornelius P. Rhoads Memorial Award Lecture. Cancer Res. *58*, 5633–5636.

Descargues, P., Sil, A.K., and Karin, M. (2008). IKKalpha, a critical regulator of epidermal differentiation and a suppressor of skin cancer. EMBO J. *27*, 2639–2647.

Esquela-Kerscher, A., and Slack, F.J. (2006). Oncomirs - microRNAs with a role in cancer. Nat. Rev. Cancer *6*, 259–269.

Fuchs, E., and Raghavan, S. (2002). Getting under the skin of epidermal morphogenesis. Nat. Rev. Genet. *3*, 199–209.

Garzon, R., Marcucci, G., and Croce, C.M. (2010). Targeting microRNAs in cancer: rationale, strategies and challenges. Nat. Rev. Drug Discov. *9*, 775–789.

González-García, A., Pritchard, C.A., Paterson, H.F., Mavria, G., Stamp, G., and Marshall, C.J. (2005). RalGDS is required for tumor formation in a model of skin carcinogenesis. Cancer Cell *7*, 219–226.

Groszer, M., Erickson, R., Scripture-Adams, D.D., Lesche, R., Trumpp, A., Zack, J.A., Kornblum, H.I., Liu, X., and Wu, H. (2001). Negative regulation of neural stem/progenitor cell proliferation by the Pten tumor suppressor gene in vivo. Science *294*, 2186–2189.

Guertin, D.A., and Sabatini, D.M. (2007). Defining the role of mTOR in cancer. Cancer Cell *12*, 9–22.

Hambardzumyan, D., Becher, O.J., Rosenblum, M.K., Pandolfi, P.P., Manova-Todorova, K., and Holland, E.C. (2008). PI3K pathway regulates survival of cancer stem cells residing in the perivascular niche following radiation in medulloblastoma in vivo. Genes Dev. *22*, 436–448.

Hammell, M., Long, D., Zhang, L., Lee, A., Carmack, C.S., Han, M., Ding, Y., and Ambros, V. (2008). mirWIP: microRNA target prediction based on microRNA-containing ribonucleoprotein-enriched transcripts. Nat. Methods *5*, 813–819.

Hammond, S.M. (2006). MicroRNAs as oncogenes. Curr. Opin. Genet. Dev. *16*, 4–9.

Hardman, M.J., Sisi, P., Banbury, D.N., and Byrne, C. (1998). Patterned acquisition of skin barrier function during development. Development *125*, 1541–1552.

Hislop, N.R., Caddy, J., Ting, S.B., Auden, A., Vasudevan, S., King, S.L., Lindeman, G.J., Visvader, J.E., Cunningham, J.M., and Jane, S.M. (2008). Grhl3 and Lmo4 play coordinate roles in epidermal migration. Dev. Biol. *321*, 263–272.

Hu, Y., Baud, V., Delhase, M., Zhang, P., Deerinck, T., Ellisman, M., Johnson, R., and Karin, M. (1999). Abnormal morphogenesis but intact IKK activation in mice lacking the IKKalpha subunit of IkappaB kinase. Science *284*, 316–320.

Hui, A.B., Lenarduzzi, M., Krushel, T., Waldron, L., Pintilie, M., Shi, W., Perez-Ordonez, B., Jurisica, I., O'Sullivan, B., Waldron, J., et al. (2010). Comprehensive MicroRNA profiling for head and neck squamous cell carcinomas. Clin. Cancer Res. *16*, 1129–1139.

Inui, M., Martello, G., and Piccolo, S. (2010). MicroRNA control of signal transduction. Nat. Rev. Mol. Cell Biol. *11*, 252–263.

Ise, K., Nakamura, K., Nakao, K., Shimizu, S., Harada, H., Ichise, T., Miyoshi, J., Gondo, Y., Ishikawa, T., Aiba, A., and Katsuki, M. (2000). Targeted deletion of the H-ras gene decreases tumor formation in mouse skin carcinogenesis. Oncogene *19*, 2951–2956.

Jane, S.M., Ting, S.B., and Cunningham, J.M. (2005). Epidermal impermeable barriers in mouse and fly. Curr. Opin. Genet. Dev. *15*, 447–453.

Jaworski, M., Buchmann, A., Bauer, P., Riess, O., and Schwarz, M. (2005). B-raf and Ha-ras mutations in chemically induced mouse liver tumors. Oncogene *24*, 1290–1295.

Jhawer, M., Goel, S., Wilson, A.J., Montagna, C., Ling, Y.H., Byun, D.S., Nasser, S., Arango, D., Shin, J., Klampfer, L., et al. (2008). PIK3CA mutation/PTEN expression status predicts response of colon cancer cells to the epidermal growth factor receptor inhibitor cetuximab. Cancer Res. *68*, 1953–1961, Erratum: (2008). Cancer Res. *68*, 6859. Erratum: (2009). Cancer Res. *69*, 9156.

Jonkers, J., Meuwissen, R., van der Gulden, H., Peterse, H., van der Valk, M., and Berns, A. (2001). Synergistic tumor suppressor activity of BRCA2 and p53 in a conditional mouse model for breast cancer. Nat. Genet. *29*, 418–425.

Kalaany, N.Y., and Sabatini, D.M. (2009). Tumours with PI3K activation are resistant to dietary restriction. Nature *458*, 725–731.

Khavari, T.A., and Rinn, J. (2007). Ras/Erk MAPK signaling in epidermal homeostasis and neoplasia. Cell Cycle *6*, 2928–2931.

Koster, M.I. (2009). Making an epidermis. Ann. N Y Acad. Sci. *1170*, 7–10.

Leemans, C.R., Braakhuis, B.J.M., and Brakenhoff, R.H. (2011). The molecular biology of head and neck cancer. Nat. Rev. Cancer *11*, 9–22.

Li, J., Yen, C., Liaw, D., Podsypanina, K., Bose, S., Wang, S.I., Puc, J., Miliaresis, C., Rodgers, L., McCombie, R., et al. (1997). PTEN, a putative protein tyrosine phosphatase gene mutated in human brain, breast, and prostate cancer. Science *275*, 1943–1947.

Liu, B., Park, E., Zhu, F., Bustos, T., Liu, J., Shen, J., Fischer, S.M., and Hu, Y. (2006). A critical role for I kappaB kinase alpha in the development of human and mouse squamous cell carcinomas. Proc. Natl. Acad. Sci. USA *103*, 17202–17207.

Liu, B., Xia, X., Zhu, F., Park, E., Carbajal, S., Kiguchi, K., DiGiovanni, J., Fischer, S.M., and Hu, Y. (2008). IKKalpha is required to maintain skin homeostasis and prevent skin cancer. Cancer Cell *14*, 212–225.

Ma, X.M., and Blenis, J. (2009). Molecular mechanisms of mTOR-mediated translational control. Nat. Rev. Mol. Cell Biol. *10*, 307–318.

Mace, K.A., Pearson, J.C., and McGinnis, W. (2005). An epidermal barrier wound repair pathway in *Drosophila* is mediated by grainy head. Science *308*, 381–385.

Maeda, G., Chiba, T., Kawashiri, S., Satoh, T., and Imai, K. (2007). Epigenetic inactivation of IkappaB Kinase-alpha in oral carcinomas and tumor progression. Clin. Cancer Res. *13*, 5041–5047.

Maehama, T., and Dixon, J.E. (1998). The tumor suppressor, PTEN/MMAC1, dephosphorylates the lipid second messenger, phosphatidylinositol 3,4,5-trisphosphate. J. Biol. Chem. *273*, 13375–13378.

Manning, B.D., and Cantley, L.C. (2007). AKT/PKB signaling: navigating downstream. Cell *129*, 1261–1274.

Mao, J.H., To, M.D., Perez-Losada, J., Wu, D., Del Rosario, R., and Balmain, A. (2004). Mutually exclusive mutations of the Pten and ras pathways in skin tumor progression. Genes Dev. *18*, 1800–1805.

Meng, F., Henson, R., Wehbe-Janek, H., Ghoshal, K., Jacob, S.T., and Patel, T. (2007). MicroRNA-21 regulates expression of the PTEN tumor suppressor gene in human hepatocellular cancer. Gastroenterology *133*, 647–658.

Ming, M., and He, Y.Y. (2009). PTEN: new insights into its regulation and function in skin cancer. J. Invest. Dermatol. *129*, 2109–2112.

Myers, M.P., Pass, I., Batty, I.H., Van der Kaay, J., Stolarov, J.P., Hemmings, B.A., Wigler, M.H., Downes, C.P., and Tonks, N.K. (1998). The lipid

phosphatase activity of PTEN is critical for its tumor supressor function. Proc. Natl. Acad. Sci. USA *95*, 13513–13518.

Nguyen, S.T., Hasegawa, S., Tsuda, H., Tomioka, H., Ushijima, M., Noda, M., Omura, K., and Miki, Y. (2007). Identification of a predictive gene expression signature of cervical lymph node metastasis in oral squamous cell carcinoma. Cancer Sci. *98*, 740–746.

Park, E., Zhu, F., Liu, B., Xia, X., Shen, J., Bustos, T., Fischer, S.M., and Hu, Y. (2007). Reduction in IkappaB kinase alpha expression promotes the development of skin papillomas and carcinomas. Cancer Res. *67*, 9158–9168.

Repasky, G.A., Chenette, E.J., and Der, C.J. (2004). Renewing the conspiracy theory debate: does Raf function alone to mediate Ras oncogenesis? Trends Cell Biol. *14*, 639–647.

Rickman, D.S., Millon, R., De Reynies, A., Thomas, E., Wasylyk, C., Muller, D., Abecassis, J., and Wasylyk, B. (2008). Prediction of future metastasis and molecular characterization of head and neck squamous-cell carcinoma based on transcriptome and genome analysis by microarrays. Oncogene *27*, 6607–6622.

Ridky, T.W., and Khavari, P.A. (2004). Pathways sufficient to induce epidermal carcinogenesis. Cell Cycle *3*, 621–624.

Rogers, H.W., Weinstock, M.A., Harris, A.R., Hinckley, M.R., Feldman, S.R., Fleischer, A.B., and Coldiron, B.M. (2010). Incidence estimate of nonmelanoma skin cancer in the United States, 2006. Arch. Dermatol. *146*, 283–287.

Salmena, L., Carracedo, A., and Pandolfi, P.P. (2008). Tenets of PTEN tumor suppression. Cell *133*, 403–414.

Scholl, F.A., Dumesic, P.A., Barragan, D.I., Harada, K., Bissonauth, V., Charron, J., and Khavari, P.A. (2007). Mek1/2 MAPK kinases are essential for Mammalian development, homeostasis, and Raf-induced hyperplasia. Dev. Cell *12*, 615–629.

Segrelles, C., Lu, J., Hammann, B., Santos, M., Moral, M., Cascallana, J.L., Lara, M.F., Rho, O., Carbajal, S., Traag, J., et al. (2007). Deregulated activity of Akt in epithelial basal cells induces spontaneous tumors and heightened sensitivity to skin carcinogenesis. Cancer Res. *67*, 10879–10888.

Selbach, M., Schwanhäusser, B., Thierfelder, N., Fang, Z., Khanin, R., and Rajewsky, N. (2008). Widespread changes in protein synthesis induced by microRNAs. Nature *455*, 58–63.

Stambolic, V., Suzuki, A., de la Pompa, J.L., Brothers, G.M., Mirtsos, C., Sasaki, T., Ruland, J., Penninger, J.M., Siderovski, D.P., and Mak, T.W. (1998). Negative regulation of PKB/Akt-dependent cell survival by the tumor suppressor PTEN. Cell *95*, 29–39.

Sundberg, J.P., Sundberg, B.A., and Beamer, W.G. (1997). Comparison of chemical carcinogen skin tumor induction efficacy in inbred, mutant, and hybrid strains of mice: morphologic variations of induced tumors and absence of a papillomavirus cocarcinogen. Mol. Carcinog. *20*, 19–32.

Suzuki, A., Itami, S., Ohishi, M., Hamada, K., Inoue, T., Komazawa, N., Senoo, H., Sasaki, T., Takeda, J., Manabe, M., et al. (2003). Keratinocyte-specific Pten deficiency results in epidermal hyperplasia, accelerated hair follicle morphogenesis and tumor formation. Cancer Res. *63*, 674–681.

Takeda, K., Takeuchi, O., Tsujimura, T., Itami, S., Adachi, O., Kawai, T., Sanjo, H., Yoshikawa, K., Terada, N., and Akira, S. (1999). Limb and skin abnormalities in mice lacking IKKalpha. Science *284*, 313–316.

Ting, S.B., Wilanowski, T., Auden, A., Hall, M., Voss, A.K., Thomas, T., Parekh, V., Cunningham, J.M., and Jane, S.M. (2003). Inositol- and folate-resistant neural tube defects in mice lacking the epithelial-specific factor Grhl-3. Nat. Med. *9*, 1513–1519.

Ting, S.B., Caddy, J., Hislop, N., Wilanowski, T., Auden, A., Zhao, L.L., Ellis, S., Kaur, P., Uchida, Y., Holleran, W.M., et al. (2005). A homolog of *Drosophila grainy head* is essential for epidermal integrity in mice. Science *308*, 411–413.

Venkatesan, K., McManus, H.R., Mello, C.C., Smith, T.F., and Hansen, U. (2003). Functional conservation between members of an ancient duplicated transcription factor family, LSF/Grainyhead. Nucleic Acids Res. *31*, 4304–4316.

Volinia, S., Calin, G.A., Liu, C.G., Ambs, S., Cimmino, A., Petrocca, F., Visone, R., Iorio, M., Roldo, C., Ferracin, M., et al. (2006). A microRNA expression signature of human solid tumors defines cancer gene targets. Proc. Natl. Acad. Sci. USA *103*, 2257–2261.

Watt, F.M. (2001). Stem cell fate and patterning in mammalian epidermis. Curr. Opin. Genet. Dev. *11*, 410–417.

Wetmore, C. (2003). Sonic hedgehog in normal and neoplastic proliferation: insight gained from human tumors and animal models. Curr. Opin. Genet. Dev. *13*, 34–42.

Wilanowski, T., Tuckfield, A., Cerruti, L., O'Connell, S., Saint, R., Parekh, V., Tao, J., Cunningham, J.M., and Jane, S.M. (2002). A highly conserved novel family of mammalian developmental transcription factors related to *Drosophila grainyhead*. Mech. Dev. *114*, 37–50.

Wilanowski, T., Caddy, J., Ting, S.B., Hislop, N.R., Cerruti, L., Auden, A., Zhao, L.L., Asquith, S., Ellis, S., Sinclair, R., et al. (2008). Perturbed desmosomal cadherin expression in grainy head-like 1-null mice. EMBO J. *27*, 886–897.

Yao, D., Alexander, C.L., Quinn, J.A., Porter, M.J., Wu, H., and Greenhalgh, D.A. (2006). PTEN loss promotes rasHa-mediated papillomatogenesis via dual up-regulation of AKT activity and cell cycle deregulation but malignant conversion proceeds via PTEN-associated pathways. Cancer Res. *66*, 1302–1312.

Yu, Z., Lin, K.K., Bhandari, A., Spencer, J.A., Xu, X., Wang, N., Lu, Z., Gill, G.N., Roop, D.R., Wertz, P., and Andersen, B. (2006). The Grainyhead-like epithelial transactivator Get-1/Grhl3 regulates epidermal terminal differentiation and interacts functionally with LMO4. Dev. Biol. *299*, 122–136.